

IR physics from the holographic RG flow

Chanyong Park^{a*} and Jung Hun Lee^{b†}

^a *Department of Physics and Photon Science, Gwangju Institute of Science and Technology,
Gwangju 61005, Korea*

^b *College of General Education, Kookmin University, Seoul, 02707, Korea*

ABSTRACT

We use the holographic method to investigate an RG flow and IR physics of a two-dimensional conformal field theory (CFT) deformed by a relevant scalar operator. On the dual gravity side, a renormalization group (RG) flow from a UV to IR CFT can be described by rolling a scalar field from an unstable to a stable equilibrium point. After considering a simple scalar potential allowing several local equilibrium points, we study the change of a coupling constant and ground state from the momentum-space and real-space RG flow viewpoints. For the real-space RG flow, we calculate the entanglement entropy as a function of a coupling constant and then explicitly show that the entanglement entropy diverges logarithmically at fixed points due to the restoration of conformal symmetry. We further study how the change of a ground state affects the two-point function and conformal dimension of a local operator numerically and analytically in the probe limit.

*e-mail : cyong21@gist.ac.kr

†e-mail : junghun.lee@kookmin.ac.kr

Contents

1	Introduction	1
2	Holographic dual of the RG flow	3
3	Holographic dual of an RG flow from a UV to IR fixed point	4
3.1	Dual QFT from the momentum-space RG flow point of view	6
3.2	Dual QFT from the real-space RG flow point of view	12
4	Anomalous dimension of a local operator in the probe limit	15
5	Discussion	19

1 Introduction

After the holography proposal, there were many attempts to understand various strongly interacting systems on the dual gravity theory side. This holographic relation or AdS/CFT correspondence becomes manifest for large supersymmetric theories like $N = 4$ Super Yang-Mills theory and ABJM theory [1–7]. In these cases, IR physics is trivial because of the conformal symmetry. One needs to break the conformal symmetry to investigate nontrivial IR physics holographically. In this work, we consider a relevant deformation to conformal field theory (CFT) and explore new macroscopic features at the IR fixed point by applying the holographic method.

Holography is one of the useful techniques for understanding strongly interacting systems. Although the dual gravity theories of maximally supersymmetric gauge theories have been known, finding the dual gravity of non-supersymmetric theories appearing in nuclear and condensed matter physics remains an unresolved issue. Nevertheless, once one can see the dual gravity theories of real physical systems, one gets more information about new physics laws governing real systems in the IR region. Since a relevant deformation breaks the conformal symmetry, it usually generates a nontrivial renormalization group (RG) flow and may allow a new IR CFT. In this case, the appearance of the IR CFT is due to the nonperturbative RG flow, including all quantum corrections. In the traditional quantum field theory (QFT), unfortunately, it is very difficult to figure out such a nonperturbative RG flow. However, one can investigate a nonperturbative RG flow by applying the holographic method [8–21]. To describe nonperturbative RG flow, there are two different descriptions, momentum-space and real-space RG flows. While an RG scale in the momentum-space RG flow is determined by the boundary position in the bulk, it is associated with a subsystem size in the real space-space RG flow.

In this work, we investigate a nonperturbative RG flow from the dual gravity point of view by using the momentum-space and real-space RG flow descriptions.

Recently, quantum entanglement entropy has been widely studied in high energy physics as well as quantum information and condensed matter theory [22–31]. The entanglement entropy is one of the important quantities to characterize the quantum correlation between subregions and plays the role of an order parameter in quantum phase transitions [32, 33]. It was well known that the entanglement entropy in the UV limit shows a universal feature proportional to the area of the entangling surface [34, 35]. For two-dimensional CFT, in particular, the entanglement entropy diverges logarithmically, and the coefficient of the logarithmic divergence corresponds to the central charge of CFT. In the holography studies, it was proposed that the entanglement entropy can be described by the area of a minimal surface extending to the dual geometry [22, 23, 36]. It was also shown that the holographic method correctly reproduces the area law of the entanglement entropy in the UV limit. At a phase transition point in the IR region, another logarithmic divergence can occur due to the restoration of a conformal symmetry. This is also true at an IR fixed point. To see this, we consider a three-dimensional Einstein-scalar gravity theory having several local extrema. In this case, a geometric solution interpolating a local maximum to minimum describes an RG flow of a dual two-dimensional QFT from a UV to IR fixed point. On this interpolating geometry, we investigate the RG flow of the entanglement entropy, which is crucially associated with the change of a ground state. After numerically studying a nonperturbative β -function, c -function, and the entanglement entropy along the RG flow, we further investigate their analytic structure near the IR fixed point. We show that the entanglement entropy diverges logarithmically at an IR fixed point and that the c -function representing the degrees of freedom monotonically decreases as a coupling constant increases along the RG flow.

We further investigate the correlation function of an additional local operator when the ground state changes along the RG flow. According to the AdS/CFT correspondence, it was proposed that a geodesic length $L(t, x_1; t, x_2)$ connecting two local operators at the boundary is related to a two-point function [3, 37–47]

$$\langle O(t, x_1) O(t, x_2) \rangle \sim e^{-\Delta_{UV} L(t, x_1; t, x_2)/R_{UV}}, \quad (1.1)$$

where Δ_{UV} means a conformal dimension of a local operator $O(t, x_1)$ at a UV fixed point. This holographic prescription describes a two-point function of the dual QFT in the probe limit. The change of a ground state with the variation of a coupling constant can affect such a two-point function by modifying the conformal dimension, which we call an anomalous dimension. We investigate how the change of the ground state leads to the variation of a conformal dimension numerically in the entire energy range and look into an anomalous dimension analytically near the IR fixed point. We also

show that the analytic prescription near the IR fixed point is perfectly matched to the nonperturbative numerical result.

The rest of this paper is organized as follows. In Sec. 2, we take into account a dual gravity theory, which realizes the RG flow from a UV to an IR fixed point. We investigate the change of a coupling constant and ground state along the RG flow from the momentum-space and real-space RG flow point of view. We show that these two different descriptions lead to the same results at fixed points. In Sec. 3, we study how the change of the ground state affects the two-point function and conformal dimension of a local operator in the probe limit. We conclude this work with some discussions in Sec. 4.

2 Holographic dual of the RG flow

Let us begin with discussing the universal features of two-dimensional QFT at critical points where a scaling symmetry is restored [35, 48–50]. We take into account a transverse field Ising model whose Hamiltonian is given by

$$H_I = - \sum_{n=1}^{L-1} \sigma_n^x - g \sum_{n=1}^{L-1} \sigma_n^z \sigma_{n+1}^z, \quad (2.1)$$

where σ_n indicates the Pauli matrices at the site n . For $g = 0$, the transverse field Ising model describes paramagnet with $\langle \sigma_n^z \rangle = 0$, while ferromagnet with $\langle \sigma_n^z \rangle = \pm 1$ appears as a ground state for $g = \infty$. Intriguingly, this model allows a second-order phase transition at $g = 1$ where the paramagnet changes into ferromagnet or vice versa. This shows that a ground state can change as a coupling constant varies. To understand these nonperturbative phenomena, we need to introduce appropriate physical quantities expressing nonperturbative features. One of those quantities is the entanglement entropy, which measures the entanglement of the ground state and plays the role of a generating functional for the real space RG flow.

The coupling constant dependence of nonperturbative physics can be described by the RG flow of the entanglement entropy. In the transverse field Ising model, the ground state for $g = 0$ is not degenerate, so the entanglement entropy automatically vanishes. For $g = \infty$, on the other hand, the ground state allows two accessible configurations with opposite signs of magnetization and results in a nonvanishing entanglement entropy proportional to $\log 2$. For a finite value of the coupling constant,

one can obtain the following entanglement entropy by applying the corner transfer matrix method [35]

$$\begin{aligned}
S_E &= \epsilon \sum_{j=0}^{\infty} \frac{2j+1}{1+e^{(2j+1)\epsilon}} + \sum_{j=0}^{\infty} \log(1+e^{-(2j+1)\epsilon}) \quad \text{for } g < 1, \\
&= \epsilon \sum_{j=0}^{\infty} \frac{2j}{1+e^{2j\epsilon}} + \sum_{j=0}^{\infty} \log(1+e^{-2j\epsilon}) \quad \text{for } g > 1,
\end{aligned} \tag{2.2}$$

with the energy gap between energy levels

$$\epsilon = \pi \frac{K(\sqrt{1-1/g^2})}{K(1/g)}, \tag{2.3}$$

where $K(1/g)$ is a complete elliptic integral of the first kind. Near the critical point at $g = 1$, the entanglement entropy is approximated by

$$S_E \approx -\frac{1}{12} \log\left(1 - \frac{1}{g}\right), \tag{2.4}$$

and leads to a logarithmic divergence at $g = 1$. In this case, the logarithmic divergence originated from the scale symmetry, which naturally appears at a second-order phase transition. This is a typical feature of two-dimensional QFTs. For higher dimensional QFTs, however, a scaling symmetry leads to a power-law divergence instead of a logarithmic one. For two-dimensional QFTs, the relation between a logarithmic divergence and scale symmetry becomes manifest when we consider other critical points. For instance, it was also well known that the entanglement entropy gives rise to another logarithmic divergence at a UV fixed point. This is also true at IR fixed points, as will be seen later, where a new nonperturbative ground state occurs with restoring a scaling symmetry. As shown here, the entanglement entropy is one of the good quantities detecting the nonperturbative change of a ground state. Nevertheless, it is not easy to calculate the nonperturbative entanglement entropy for interacting QFTs. In this work, we investigate the RG flow of the entanglement entropy holographically by studying the change of a ground state.

3 Holographic dual of an RG flow from a UV to IR fixed point

We take into account a two-dimensional CFT deformed by a relevant operator. Even when a UV theory is weakly interacting, IR physics triggered by a relevant deformation can strongly interact. Therefore, knowing IR physics requires understanding a nonperturbative RG flow. To study such a nonperturbative RG flow in the holographic setup, we consider a three-dimensional gravity theory with a bulk scalar field

$$S = \frac{1}{16\pi G} \int d^3 X \sqrt{-g} \left(\mathcal{R} - \frac{1}{2} \partial_M \phi \partial^M \phi - \frac{V(\phi)}{R_{UV}^2} \right). \tag{3.1}$$

To describe an RG flow from a UV CFT to a new IR CFT, we introduce the following simple scalar potential as a toy model

$$V(\phi) = 2R_{UV}^2\Lambda_{UV} + \frac{M_\phi^2}{2}\phi^2 + \frac{\lambda}{4}\phi^4 = 2R_{UV}^2\Lambda_{UV} + \frac{\lambda}{4}\phi^2 \left(\phi^2 - 2\frac{m_\phi^2}{\lambda} \right), \quad (3.2)$$

where $M_\phi^2 = -m_\phi^2 < 0$, $\lambda > 0$ and $\Lambda_{UV} = -1/R_{UV}^2$ with a UV AdS radius R_{UV} . Note that here we exploit dimensionless field ϕ and coupling constants, m_ϕ^2 and λ . The scalar potential considered here allows one local maximum, $V = -2\Lambda_{UV}$ at $\phi = 0$, and two degenerated local minima, $V = 2R_{UV}^2\Lambda_{UV} - m_\phi^4/4\lambda$ at $\phi_\pm = \pm m_\phi/\sqrt{\lambda}$.

We concentrate on the RG flow from a UV CFT to another IR CFT. Such an RG flow in the holographic setup can be realized by a geometric solution interpolating a local maximum to one of the local minima. A local maximum and minimum correspond to an unstable or stable equilibrium point on the gravity side, so the scalar field rolls down from a maximum to a minimum. In other words, a rolling motion in the gravity maps to an RG flow of the dual QFT. From now on, we take into account the RG flow from a UV CFT at $\phi = 0$ to an IR CFT at $\phi_+ = \phi_{IR}$. On the dual QFT side, the corresponding RG flow can be triggered by a relevant operator. To consider a relevant operator, we assume that the bulk scalar field has a negative mass square in the range of $0 < -M_\phi^2 = m_\phi^2 < 1$. If the bulk scalar field depends only on the radial coordinate, the boundary Lorentz symmetry is preserved. In this case, the most general metric ansatz is given by

$$ds^2 = dy^2 + e^{2A(y)}\eta_{\mu\nu}dx^\mu dx^\nu. \quad (3.3)$$

Here, UV and IR fixed points appear at $y = \infty$ and $-\infty$, respectively.

A geometric solution interpolating two fixed points is obtained by solving the following equations of motion

$$0 = A'^2 - \frac{1}{4}\phi'^2 - \frac{m_\phi^2}{4R_{UV}^2}\phi^2 + \frac{\lambda}{8R_{UV}^2}\phi^4 - \frac{1}{R_{UV}^2}, \quad (3.4)$$

$$0 = A'' + A'^2 + \frac{1}{4}\phi'^2 - \frac{m_\phi^2}{4R_{UV}^2}\phi^2 + \frac{\lambda}{8R_{UV}^2}\phi^4 - \frac{1}{R_{UV}^2}, \quad (3.5)$$

$$0 = \phi'' + 2A'\phi' + \frac{m_\phi^2}{R_{UV}^2}\phi - \frac{\lambda}{R_{UV}^2}\phi^3, \quad (3.6)$$

where the prime means a derivative with respect to the radial coordinate, y . Here, the first equation is a constraint, and the others determine the dynamics of ϕ and A . After taking $R_{UV} = 1$, $m_\phi = \sqrt{3}/2$ and $\lambda = 0.1$, we solve the above equations numerically and depict the numerical result in Fig. 1. At the UV fixed point, the result in Fig. 1 shows that the asymptotic geometry is given by an AdS space

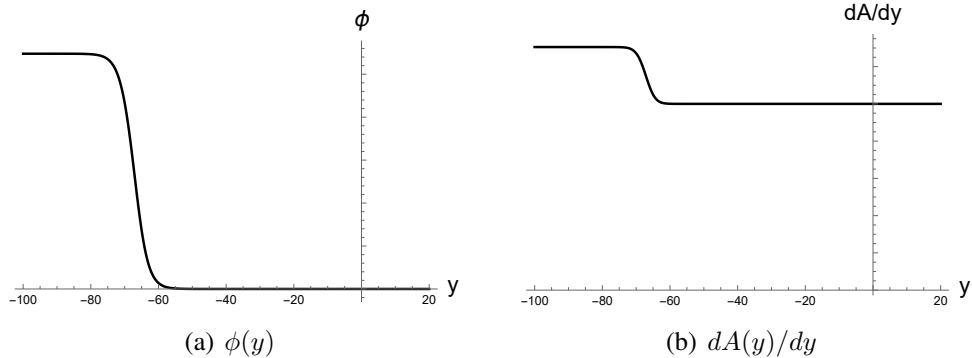


Figure 1. Profiles of (a) the scalar field $\phi(y)$ and (b) the derivative of the metric factor, $dA(y)/dy$, where we take $R_{UV} = 1$, $m_\phi = \sqrt{3}/2$ and $\lambda = 0.1$. At the UV fixed point ($y = \infty$), $\phi = 0$ and $dA/dy = 1$, whereas they are modified into $\phi = \phi_{IR} = 2.7386$ and $dA/dy = 1.3050$ at the IR fixed point ($y = -\infty$).

with $\phi = 0$ and $A(y) = y/R_{UV}$ at $y = \infty$. On the other hand, ϕ and A' approach $\phi_{IR} = 2.7386$ and $A' = 1.3050$ at the IR fixed point ($y = -\infty$) which again leads to another AdS space, $A(y) = y/R_{IR}$ at $y = -\infty$ with a new IR AdS radius $R_{IR} = 0.7663 R_{UV}$. In the holographic study, these two UV and IR AdS spaces are mapped to UV and IR fixed points of the dual QFT where a conformal symmetry is restored with vanishing β -functions.

3.1 Dual QFT from the momentum-space RG flow point of view

Above, we studied the geometric solution interpolating unstable and stable equilibrium points. According to the holography, it can be reinterpreted as an RG flow from a UV to IR fixed point. This feature can be clarified by two different holographic descriptions, momentum-space and real-space RG flows. We first discuss the dual of the interpolating geometry from the momentum-space RG flow point of view.

When the scalar field is absent, the previous gravity theory allows an AdS space as an exact solution. Since the isometry of an AdS space is equivalent to the conformal symmetry of the dual QFT, a $(d + 1)$ -dimensional AdS space is mapped to the ground state of a d -dimensional CFT. Therefore, the above interpolating geometry can be regarded as the deformation of the CFT. For $0 < m_\phi^2 < 1$, the bulk field ϕ rapidly suppresses in the asymptotic region ($y \rightarrow \infty$) and the effect of $\lambda\phi^4$ becomes negligible. As a result, the metric factor is well approximated by the AdS one, $A(y) = y/R_{UV}$, which is the dual of a UV CFT. Introducing a new radial coordinate z to describe UV physics

$$z = R_{UV} e^{-y/R_{UV}}, \tag{3.7}$$

the asymptotic geometry ($z \rightarrow 0$) can be described by

$$ds_{UV}^2 = \frac{R_{UV}^2}{z^2} (-dt^2 + dx^2 + dz^2). \quad (3.8)$$

Ignoring $\lambda\phi^4$ in the asymptotic region, the scalar field is governed by

$$0 = \partial_z^2 \phi - \frac{1}{z} \partial_z \phi + \frac{m_\phi^2}{z^2} \phi, \quad (3.9)$$

and gives rise to the following profile

$$\phi(z) = c_1 z^{2-\Delta_{UV}} + c_2 z^{\Delta_{UV}}, \quad (3.10)$$

where a conformal dimension of a dual scalar operator is given by

$$\Delta_{UV} = 1 + \sqrt{1 - m_\phi^2}. \quad (3.11)$$

It is worth noting that the conformal dimension in an alternative quantization is defined as $2 - \Delta_{UV}$ instead of Δ_{UV} .

Denoting a dual operator of the bulk field ϕ as O_ϕ , it can be classified into a relevant, irrelevant, and marginal operator depending on its conformal dimension [15]. This classification is associated with the scalar field mass in the bulk and a β -function on the dual QFT side. If the conformal dimension is less than the spacetime dimension, $\Delta < d$, we call it a relevant operator. In the dual gravity theory, it constrains the scalar field mass to be in $M_\phi^2 < 0$. On the dual QFT side, it is associated with a negative β -function

$$\beta_\phi = -(d - \Delta_{UV})\phi < 0. \quad (3.12)$$

On the other hand, the conformal dimension of an irrelevant operator has $\Delta > d$, which gives rise to $M_\phi^2 > 0$ and $\beta_\phi > 0$. For $\Delta = d$, lastly, it becomes a marginal operator which leads to $M_\phi^2 = 0$ and $\beta_\phi = 0$. In the previous gravity theory, since we took into account the case with $-1 < M_\phi^2 = -m_\phi^2 < 0$, the dual operator O_ϕ is given by a relevant operator with $\Delta_{UV} < 2$. Although the effect of a relevant deformation is negligible in the UV region, it can significantly modify IR physics due to nonperturbative quantum corrections.

According to the AdS/CFT correspondence, the on-shell gravity action can be regarded as a quantum partition function of the dual QFT

$$e^{iS_{gravity}[\phi(\bar{y})]} = \left\langle e^{i \int d^2x \phi O_\phi} \right\rangle_{QFT} = e^{i\Gamma[\phi(\mu); \mu]}, \quad (3.13)$$

where \bar{y} and μ mean a position of the boundary in the bulk and the RG scale of the dual QFT. Here, $\Gamma[g(\mu); \mu]$ indicates a generating functional of the dual QFT. Following this relation, we can connect the previous interpolating geometry to an RG flow with a nontrivial β -function. To do so, we first need to relate the RG scale to the boundary position in the bulk. In the normal coordinate system (3.3), since the scale transformation of the boundary coordinates is related to the translation in the bulk, the RG transformation of the dual QFT can be described by the shift of the boundary. Therefore, the RG scale μ is connected to the boundary position \bar{y} in the bulk

$$\mu = e^{A(\bar{y})}/R_{UV}. \quad (3.14)$$

Near the UV fixed point, the RG scale is approximately described by $\mu \sim 1/z$.

Now, we identify the value of the scalar field at the boundary, $\phi(\bar{y})$, with a coupling constant of the deformation operator O_ϕ on the dual QFT side. From the previous interpolating geometry, then, we can understand the RG flow of its dual QFT. Near the UV fixed point, the asymptotic solution in (3.10) results in

$$\beta_\phi = \mu \frac{d\phi}{d\mu} = -(2 - \Delta_{UV})\phi + \dots < 0, \quad (3.15)$$

where the ellipsis implies higher-order small quantum corrections. Since we took into account a relevant deformation, the β -function in (3.15) becomes negative. This β -function determines the coupling constant ϕ as a function of the RG scale

$$\phi \sim \mu^{-(2-\Delta_{UV})} + \dots, \quad (3.16)$$

Since the coupling constant approaches zero at the UV fixed point ($\mu \rightarrow \infty$), the perturbative description is possible. As a result, the ground state in the high-energy region is described by a perturbative vacuum. In the IR limit, on the other hand, the coupling constant increases along the RG flow, so the quantum corrections become significant and do not allow the perturbation anymore. This indicates that to understand IR physics, we need to specify a nonperturbative ground state. Since we have no nonperturbative analytic method in the traditional QFT, the holographic study would help figure out nonperturbative IR physics. Using the scalar field profile and interpolating solution in Fig. 1, a nonperturbative β -function can be reexpressed in terms of the dual gravity quantities

$$\beta_\phi = \mu \frac{d\phi}{d\mu} = \frac{d\phi(\bar{y})/d\bar{y}}{dA(\bar{y})/d\bar{y}}. \quad (3.17)$$

Another important quantity characterizing CFTs is a central charge, which measures the degrees of freedom. In the momentum-space RG flow, a c -function is given by [18, 51, 52]

$$c = \frac{3}{2G} \frac{1}{A'}, \quad (3.18)$$

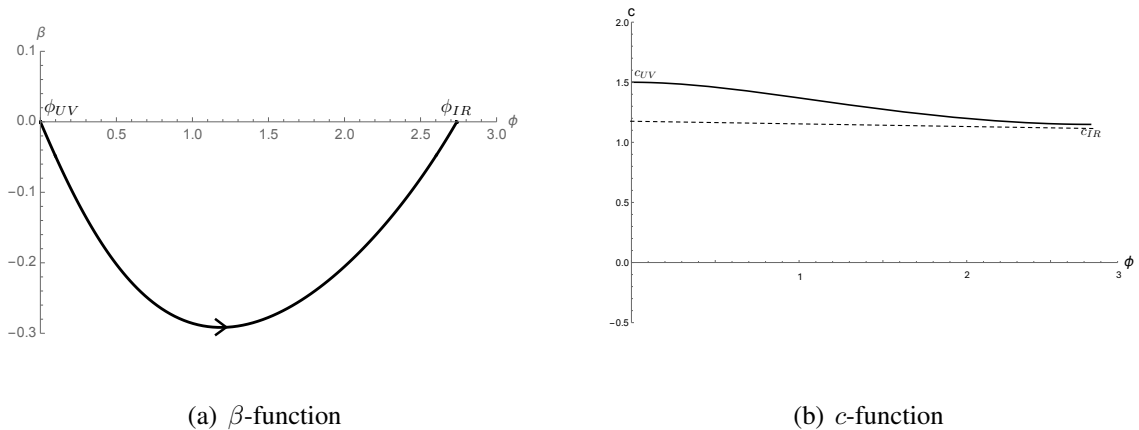


Figure 2. From the previous interpolating geometry, we derive nonperturbative (a) β -function and (b) c -function of the dual QFT, where we take $m_\phi = \sqrt{3}/2$, $\lambda = 0.1$ and $G = R_{UV} = 1$. Note that since A'' is manifestly negative, the c -function monotonically decreases along the RG flow [18].

where G is a Newton constant of a three-dimensional gravity theory. In Fig.2, we numerically plot the β -function and c -function as functions of the coupling constant. The numerical result in Fig. 2 (a) shows that there exists an IR fixed point at $\phi = \phi_{IR}$ with a vanishing β -function and that the β -function is always negative during the RG flow. Fig. 2 (b) shows that the degrees of freedom reduce as the coupling constant increases along the RG flow.

To understand IR physics more, we further perform analytic analysis near the IR fixed point. Due to the restoration of the conformal symmetry at the IR fixed point, the dual geometry in the low energy limit ($y \rightarrow -\infty$) is again given by another AdS space. This IR geometry corresponds to the ground state of an IR CFT. The IR ground state is nonperturbative because it contains all quantum corrections after the RG flow. Therefore, the IR ground state is usually different from the perturbative one defined in the UV region. If we represent the IR geometry as $A(y) = y/R_{IR}$ with an IR AdS radius, which will be determined later, the IR metric becomes

$$ds_{IR}^2 = \frac{R_{IR}^2}{\bar{z}^2} (-d\bar{t}^2 + d\bar{x}^2 + d\bar{z}^2), \quad (3.19)$$

where a new IR coordinate \bar{z} is related to y

$$\bar{z} = R_{IR} e^{-y/R_{IR}}. \quad (3.20)$$

This IR metric is valid only for $\bar{z} \rightarrow \infty$. Comparing (3.7) and (3.20), the UV coordinates can be related to the IR ones

$$z = \frac{R_{UV}}{R_{IR}^{R_{IR}/R_{UV}}} \bar{z}^{R_{IR}/R_{UV}}, \quad dt = \frac{R_{IR}^{R_{UV}-R_{IR}}}{\bar{z}^{R_{UV}-R_{IR}}} d\bar{t} \quad \text{and} \quad dx = \frac{R_{IR}^{R_{UV}-R_{IR}}}{\bar{z}^{R_{UV}-R_{IR}}} d\bar{x}. \quad (3.21)$$

From the dual QFT point of view, the first relation describes the change in the RG scale, and the remaining two relations describe the rescaling of the boundary coordinates along the RG flow.

Now, we investigate IR physics in terms of a new coordinate \bar{z} . As shown in Fig. 2, an IR fixed point occurs at $\phi = \phi_{IR}$, which provides a new nonperturbative ground state. Nevertheless, the restoration of the conformal symmetry at the IR fixed point still allows us to exploit the conformal perturbation around the nonperturbative IR ground state. From the scalar potential in (3.2), the IR fixed point is determined in terms of the bulk couplings

$$\phi_{IR} = m_\phi / \sqrt{\lambda}. \quad (3.22)$$

Expanding the scalar field with a small fluctuation $\delta\phi$

$$\phi = \phi_{IR} + \delta\phi, \quad (3.23)$$

the scalar potential becomes near the IR fixed point

$$V \approx -2 \left(\frac{8\lambda + m_\phi^4}{8\lambda} \right) + m_\phi^2 \delta\phi^2, \quad (3.24)$$

where an IR cosmological constant is given by

$$\Lambda_{IR} = - \left(\frac{8\lambda + m_\phi^4}{8\lambda} \right) \frac{1}{R_{UV}^2}. \quad (3.25)$$

Therefore, the IR AdS radius R_{IR} is related to the UV one

$$R_{IR} = \sqrt{\frac{8\lambda}{8\lambda + m_\phi^4}} R_{UV}. \quad (3.26)$$

Applying the numerical values used in Fig. 1, the analytic formulas in (3.22) and (3.26) reproduce the results of Fig. 1, $\phi_{IR} = 2.7386$ and $R_{IR} = 0.7663$.

Applying this formula to the previous interpolating geometry, the central charges of the UV and IR CFTs are reduced to

$$c_{UV} = \frac{3R_{UV}}{2G} \quad \text{with} \quad c_{IR} = \frac{3R_{IR}}{2G} = \sqrt{\frac{8\lambda}{8\lambda + m_\phi^4}} c_{UV}. \quad (3.27)$$

Here, the IR central charge characterizing the IR CFT is different from the UV one. Moreover, recalling that the IR AdS radius is always smaller than the UV one ($R_{IR} < R_{UV}$), we see that c_{UV} is always larger than c_{IR} , which is consistent with the c -theorem. As a result, the degrees of freedom

of the nonperturbative IR ground state are less than those of the perturbative vacuum at the UV fixed point.

Due to the restoration of the conformal symmetry at the IR fixed point, the dual geometry is again given by an AdS space in (3.19). To determine the ϕ 's profile near the IR fixed point, we take into account a small fluctuation $\delta\phi$, whose equation of motion becomes

$$0 = \partial_{\bar{z}}^2 \delta\phi - \frac{1}{\bar{z}} \partial_{\bar{z}} \delta\phi - \frac{2 m_\phi^2 R_{IR}^2}{\bar{z}^2 R_{UV}^2} \delta\phi. \quad (3.28)$$

The solution of this equation reads

$$\delta\phi = d_1 \bar{z}^{2+\delta_{IR}} - d_2 \bar{z}^{-\delta_{IR}}, \quad (3.29)$$

where d_1 and d_2 are two integral constants and δ_{IR} is given by

$$\delta_{IR} = \frac{\sqrt{8\lambda + m_\phi^4 + 16m_\phi^2\lambda}}{\sqrt{8\lambda + m_\phi^4}} - 1. \quad (3.30)$$

In this case, since $\delta_{IR} > 0$, $\delta\phi$ diverges as $\bar{z} \rightarrow \infty$. However, we assumed at the early stage that ϕ has a finite value ϕ_{IR} at the IR fixed point, so the first term in (3.29) must vanish to have a finite value ϕ_{IR} . This implies that we have to take $d_1 = 0$. Then, the resulting profile of ϕ near the IR fixed point yields

$$\phi(\bar{z}) = \phi_{IR} - d_2 \bar{z}^{-\delta_{IR}} + \dots, \quad (3.31)$$

where d_2 is given by a function of c_1 and c_2 in (3.10).

Exploiting the scalar profile in the IR region, we can determine the IR RG scale as a function of the coupling constant

$$\mu \sim \frac{1}{\bar{z}} \approx \left(\frac{\phi_{IR} - \phi(\bar{z})}{d_2} \right)^{1/\delta_{IR}}. \quad (3.32)$$

This implies that the coupling constant in the IR region is given by a function of the RG scale

$$\phi(\mu) \approx \phi_{IR} - d_2 \mu^{\delta_{IR}}. \quad (3.33)$$

Therefore, the β -function near the IR fixed point is reduced to

$$\beta_\phi = \mu \frac{d\phi}{d\mu} = -\delta_{IR} \left(\phi_{IR} - \phi(\mu) \right) + \dots. \quad (3.34)$$

This, as expected, shows that the β -function is negative and vanishes at the IR fixed point, $\phi(\mu) = \phi_{IR}$.

3.2 Dual QFT from the real-space RG flow point of view

In the previous section, we studied how to understand the interpolating geometry on the dual QFT side by applying the momentum-space RG flow. In the momentum-space RG flow, the RG flow is described by the shift of the boundary in the bulk. This is possible because the RG transformation of the dual QFT can be realized by the shift of the boundary. There is another description to understand the interpolating geometry. We first fix the boundary position at $y = \infty$ and then define the entanglement entropy between a subsystem with a size ℓ and its complement at the boundary. In this entanglement entropy description, an RG scale is described by the subsystem size instead of the boundary position. This resembles the real-space RG flow widely used in condensed matter physics. The RG flow of the entanglement entropy, as shown in the previous transverse field Ising model, can describe the change of the ground state and be used as an indicator of the restoration of the scale symmetry.

To study the change of a ground state, from now on, we concentrate on the RG flow of the entanglement entropy. To define the entanglement entropy, we first take a subsystem with a size ℓ . In the holographic setup, the entanglement entropy is determined by the area of a minimal surface extending to the dual geometry. In the previous interpolating geometry (3.3), the entanglement entropy is governed by [22, 23]

$$S_E = \frac{1}{4G} \int_{-\ell/2}^{\ell/2} dx \sqrt{y'^2 + e^{2A(y)}}, \quad (3.35)$$

where the prime means a derivative with respect to x . Using the conserved quantity, the subsystem size and entanglement entropy can be reexpressed as functions of a turning point y_t , at which $y' = 0$,

$$\ell = \int_{y_t}^{\Lambda_y} dy \frac{2}{e^{2A(y)} \sqrt{e^{-2A_t} - e^{-2A(y)}}}, \quad (3.36)$$

$$S_E = \frac{1}{2G} \int_{y_t}^{\Lambda_y} dy \frac{e^{-A_t}}{e^{2A(y)} \sqrt{e^{-2A_t} - e^{-2A(y)}}}, \quad (3.37)$$

where $A_t = A(y_t)$ and Λ_y denotes a UV cutoff. To perform these integrals numerically, we take $G = 1$, $R_{UV} = 1$, $m_\phi = \sqrt{3}/2$, $\lambda = 0.1$ and $\Lambda_y = 20$. Then, we can determine the entanglement entropy as a function of the subsystem size. Recalling that the subsystem size is also determined by the turning point y_t , the entanglement entropy can be reexpressed as a function of the turning point, which plays the RG scale of the real-space RG flow. Interpreting $\phi(y_t)$ as a coupling constant at the RG scale $\mu = e^{A(y_t)}/R_{UV}$, we depict the entanglement entropy as a function of the coupling constant in Fig. 3(a). The numerical result shows that the entanglement entropy increases logarithmically at the UV fixed point ($\phi_t = 0$), where we get rid of a UV divergence. At the IR fixed point ($\phi_t = \phi_{IR} = 2.7386$), the entanglement entropy again diverges logarithmically. This implies that a logarithmic divergence

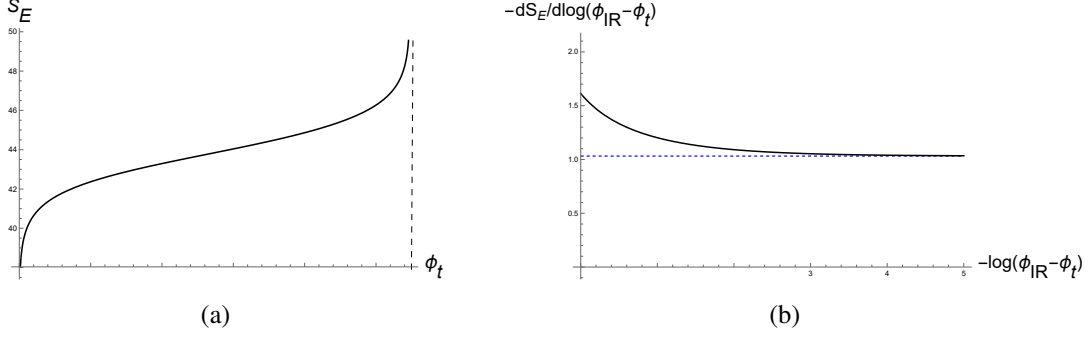


Figure 3. (a) Entanglement entropy depending on the coupling constant and (b) the coefficient of the IR entanglement entropy where we fix $G = 1$. (a) The entanglement entropy shows a logarithmic divergence at $\phi_t \rightarrow \phi_{IR}$. (b) When $-\log(\phi_{IR} - \phi_t) \rightarrow \infty$ near the IR fixed point, $-dS_E/d\log(\phi_{IR} - \phi_t)$ approaches 1.0316 which is consistent with the value expected by (3.50).

of the entanglement entropy naturally appears when the scaling symmetry is restored. The numerical result in Fig. 3(b) shows that the coefficient of the logarithmic term approaches at the IR fixed point

$$-\frac{dS_E}{d\log(\phi_{IR} - \phi_t)} = 1.0316. \quad (3.38)$$

Although we calculated the entanglement entropy numerically in Fig. 3, it is still important to know the analytic form to clarify the parameter dependence. To do so, we delve into the entanglement entropy analytically. Assuming that a subsystem has a small size ℓ , a minimal surface in the UV limit extends to only the asymptotic region. Therefore, the dominant entanglement entropy in the UV region is governed by

$$S_E \approx \frac{R_{UV}}{4G} \int_{-\ell/2}^{\ell/2} dx \frac{\sqrt{z'^2 + 1}}{z}, \quad (3.39)$$

where z is the radial coordinate of the UV AdS geometry in (3.8). To evaluate the entanglement entropy, we introduce a turning point z_t at $x = 0$, where $z' = 0$. Then, the subsystem size and entanglement entropy in the UV limit ($\ell \rightarrow 0$ and $z_t \rightarrow 0$) are reexpressed in terms of the turning point

$$\ell(z_t) = \int_0^{z_t} dz \frac{2z}{\sqrt{z_t^2 - z^2}} = 2z_t + \dots, \quad (3.40)$$

$$S_E(z_t) = \frac{R_{UV}}{2G} \int_\epsilon^{z_t} dz \frac{z_t}{z\sqrt{z_t^2 - z^2}} = \frac{R_{UV}}{2G} \log \frac{z_t}{\epsilon} + \dots, \quad (3.41)$$

where ϵ means a UV cutoff in the z coordinate. Here, the ellipses mean higher-order corrections caused by the small deformation in the asymptotic region. The entanglement entropy relying on the

subsystem size results in

$$S_E = \frac{R_{UV}}{2G} \log \frac{\ell}{\epsilon} + \mathcal{O}(\ell). \quad (3.42)$$

In this case, the leading contribution comes from a two-dimensional UV CFT with small higher-order corrections caused by the relevant deformation.

Recalling that the turning point determines the RG scale of the entanglement entropy, $\mu \sim 1/z_t \sim 1/\ell$, we can identify $\phi(z_t)$ at the turning point with the coupling constant at the RG scale μ . In the UV region, then, the turning point z_t is related to the coupling constant $\phi(z_t) = \phi_t$

$$z_t \approx \left(\frac{\phi_t}{c_1} \right)^{1/(2-\Delta_{UV})}. \quad (3.43)$$

Therefore, the entanglement entropy becomes

$$S_E = \frac{R_{UV}}{2(2-\Delta_{UV})G} \log \frac{\phi_t}{\phi_\epsilon} + \mathcal{O} \left(\phi_t^{1/(2-\Delta_{UV})} \right), \quad (3.44)$$

where $\phi_\epsilon = \phi(\epsilon)$ means the coupling constant at the UV fixed point. This explicitly shows that the entanglement entropy diverges logarithmically as the coupling constant approaches zero at the UV fixed point. For a two-dimensional real-space RG flow, a c -function is defined as

$$c = -3 \frac{dS_E}{d \log \mu}. \quad (3.45)$$

which reduces to a central charge at fixed points. At the UV fixed point, the central charge is given by

$$c_{UV} = -3 \frac{dS_E}{d \log \mu} = 3 \frac{dS_E}{d \log \ell} = \frac{3R_{UV}}{2G}. \quad (3.46)$$

Now, let us study the entanglement entropy in a large subsystem size limit ($\ell \rightarrow \infty$), which corresponds to the IR limit. The IR entanglement entropy in the holographic setup is defined as the integration over x in the range of $-\ell/2 < x < \ell/2$ so that it also contains the UV effect. Nevertheless, the leading contribution to the IR entanglement entropy comes from the minimal surface area extending to the IR region. Therefore, the entanglement entropy near the IR fixed point is approximately given by

$$S_E \approx \lim_{\ell \rightarrow \infty} \frac{R_{IR}}{4G} \int_{-\ell/2}^{\ell/2} dx \frac{\sqrt{\bar{z}'^2 + 1}}{\bar{z}}, \quad (3.47)$$

where \bar{z} is the radial coordinate of (3.19) in the IR region. Similar to the previous UV entanglement entropy, the leading subsystem size and IR entanglement entropy up to the UV divergence are

determined by the turning point

$$\ell(\bar{z}_t) \approx \lim_{z_t \rightarrow \infty} 2\bar{z}_t, \quad (3.48)$$

$$S_E(\bar{z}_t) \approx \lim_{z_t \rightarrow \infty} \frac{R_{IR}}{2G} \log(\bar{z}_t) \quad (3.49)$$

The dominant IR entanglement entropy in terms of the coupling constant becomes

$$\begin{aligned} S_E &\approx -\frac{R_{IR}}{2G\delta_{IR}} \log\left(\frac{\phi_{IR} - \bar{\phi}_t}{d_2}\right), \\ &= -\frac{\sqrt{8\lambda} R_{UV}}{2\left(\sqrt{8\lambda + m_\phi^4} + 16m_\phi^2\lambda - \sqrt{8\lambda + m_\phi^4}\right)G} \log\left(\frac{\phi_{IR} - \bar{\phi}_t}{d_2}\right). \end{aligned} \quad (3.50)$$

where $\bar{\phi}_t = \phi(\bar{z}_t)$. This shows that, similar to the previous transverse field Ising model, a logarithmic divergence appears at the IR fixed point due to the restoration of the conformal symmetry. Using the numerical values used in Fig. 1, the coefficient of the logarithmic term results in

$$-\frac{dS_E}{d\log(\phi_{IR} - \bar{\phi}_t)} = \frac{\sqrt{8\lambda} R_{UV}}{2\left(\sqrt{8\lambda + m_\phi^4} + 16m_\phi^2\lambda - \sqrt{8\lambda + m_\phi^4}\right)G} = 1.0316. \quad (3.51)$$

This is perfectly matched to the numerical result in (3.38). Recalling that the RG scale in the IR region is given by $\mu = 1/\bar{z}_t$, the central charge reads at the IR fixed point

$$c_{IR} = 3\frac{dS_E}{d\log\mu} = \frac{3R_{IR}}{2G}, \quad (3.52)$$

which are perfectly matched to the result of the momentum space RG flow in (3.27). This implies that the degrees of freedom decrease as the coupling constant becomes strong along the RG flow.

4 Anomalous dimension of a local operator in the probe limit

In the previous section, we studied how to describe the nonperturbative RG flow in the dual gravity theory. We showed that the ground state is modified as the coupling constant varies along the RG flow. Now, we investigate how the change of the ground state can affect the correlation functions of local operators. To do so, we introduce two additional local operators, $O_\chi(t_1, x_1)$ and $O_\chi(t_2, x_2)$, on the previous ground state deformed by O_ϕ . If the interaction between O_χ and O_ϕ is strong, the effect of O_χ modifies the ground state and spoils the IR fixed point studied in the previous sections. From now on, we assume that the interaction between O_χ and O_χ is weak during the RG flow. Then,

we can take into account a probe limit where the additional operator O_χ does not modify the ground state. Since the IR fixed point remains in the probe limit, we can calculate two-point functions of O_χ perturbatively. Supposed that the scalar operator O_χ has a conformal dimension Δ_{UV}^χ at the UV fixed point, then the conformal symmetry constrains its two-point function at the UV fixed point to be

$$\langle O_\chi(t_1, x_1) O_\chi(t_2, x_2) \rangle = \frac{1}{(-|t_1 - t_2|^2 + |x_1 - x_2|^2)^{\Delta_{UV}^\chi}}. \quad (4.1)$$

At the IR fixed point, the restoration of the conformal symmetry again leads to a similar two-point function with a different IR conformal dimension because nonperturbative quantum effects modify the conformal dimension of O_χ during the RG flow. In this section, we investigate with the aid of holography how the change of the ground state along the RG flow modifies the conformal dimension of O_χ in the probe limit.

In the holographic setup, it was proposed that a two-point function is described by a geodesic length connecting two local operators at the boundary [37–41, 45]

$$\langle O_\chi(t, x_1) O_\chi(t, x_2) \rangle \sim e^{-\Delta_{UV}^\chi L(t, x_1; t, x_2)/R_{UV}}, \quad (4.2)$$

where $L(t, x_1; t, x_2)$ indicates a geodesic length. Before discussing a holographic two-point function, it is worth noting that calculating a holographic two-point function for a three-dimensional gravity is similar to the entanglement entropy calculation. This is because a minimal surface for a three-dimensional gravity is given by a geodesic curve. However, this is not the case for higher dimensional gravity theories. Using the proposal in (4.2), the CFT's correlators were reproduced at zero and finite temperature [53–56].

Applying the holographic formula (4.2) to the previous interpolating geometry, the geodesic length is governed by

$$L(t, x_1; t, x_2) = \int_{x_1}^{x_2} dx \sqrt{y'^2 + e^{2A(y)}}. \quad (4.3)$$

Similar to the previous entanglement entropy calculation, we represent an operator's distance and geodesic length as functions of a turning point

$$\begin{aligned} |x_1 - x_2| &= \int_{y_t}^{\Lambda_y} dy \frac{2e^{-2A(y)}}{\sqrt{e^{-2A_t} - e^{-2A(y)}}}, \\ L(t, x_1; t, x_2) &= \int_{y_t}^{\Lambda_y} dy \frac{2e^{-A_t}}{\sqrt{e^{-2A_t} - e^{-2A(y)}}}, \end{aligned} \quad (4.4)$$

where $A_t = A(y_t)$ means the value of $A(y)$ at a turning point y_t . To study the change in the conformal dimension, we define an effective conformal dimension as

$$\Delta_{eff}(|x_1 - x_2|) \equiv -\frac{1}{2} \frac{d \log \langle O_\chi(t, x_1) O_\chi(t, x_2) \rangle}{d \log |x_1 - x_2|}. \quad (4.5)$$

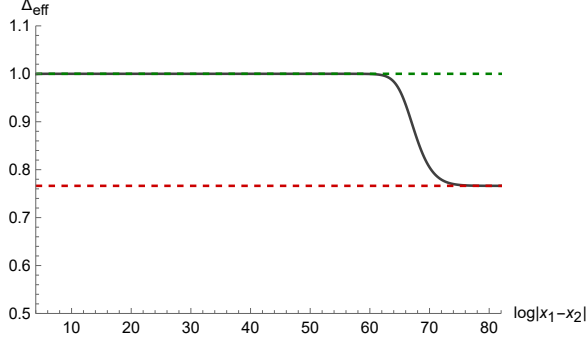


Figure 4. The RG flow of a conformal dimension of O_χ . When the ground state is deformed by O_ϕ , the change of the ground state affects another operator O_χ . Assuming that the UV conformal dimension is $\Delta_{UV}^\chi = 1$, the conformal dimension along the RG flow changes into $\Delta_{IR}^\chi = 0.7663$ at the IR fixed point. This is consistent with the previous theoretical expectation in (4.13).

The effective conformal dimension defined here is generally given by a function of the operator's distance. However, it becomes a constant at fixed points due to the scale symmetry. We plot the effective potential numerically in Fig. 4, where we take $\Delta_{UV}^\chi = 1$, $m_\phi = \sqrt{3}/2$ and $\lambda = 0.1$. The numerical simulation shows that the effective conformal dimension monotonically decreases and approaches $\Delta_{IR}^\chi = 0.7663$ at the IR fixed point. This implies that the IR conformal dimension is given by

$$\Delta_{IR}^\chi = 0.7663 \Delta_{UV}^\chi. \quad (4.6)$$

So far, we studied the change of the effective conformal dimension numerically in the real-space RG flow. To understand analytically how (4.6) appears at the IR fixed point, we investigate the conformal dimension from the momentum-space RG flow point of view. To do so, we first introduce a bulk field χ as the dual of O_χ . To realize the UV conformal dimension Δ_{UV}^χ , we assume that the mass of χ is given by $-m_\chi^2/R_{UV}^2$ in the asymptotic region. Since we consider the scalar field χ in the probe limit, its gravitational backreaction can be ignored. Then, the bulk field χ satisfies the following linear differential equation in the asymptotic region

$$\begin{aligned} 0 &= \frac{1}{\sqrt{-g}} \partial_\mu (\sqrt{-g} g^{\mu\nu} \partial_\nu \chi) + \frac{m_\chi^2}{R_{UV}^2} \chi \\ &\approx \frac{z^2}{R_{UV}^2} \left(\partial_z^2 \chi - \frac{1}{z} \partial_z \chi + \frac{m_\chi^2}{z^2} \chi \right), \end{aligned} \quad (4.7)$$

where $g_{\mu\nu}$ indicates the metric of the previous interpolating geometry. Assuming that the scalar field relies only on the radial coordinate, the mass of χ determines the profile

$$\chi = c_1 z^{2-\Delta_{UV}^\chi} + c_2 z^{\Delta_{UV}^\chi}, \quad (4.8)$$

where c_1 and c_2 are two integral constants and the dual operator O_χ has a conformal dimension

$$\Delta_{UV}^x = 1 + \sqrt{1 - m_\chi^2}. \quad (4.9)$$

In this case, it is worth noting that since χ is governed by a linear second-order differential equation, c_1 and c_2 are not mixed in the probe limit. Using the obtained UV conformal dimension, the two-point function of O_χ at the UV fixed point results in

$$\langle O_\chi(t, x_1) O_\chi(t, x_2) \rangle = \frac{1}{|x_1 - x_2|^{2\Delta_{UV}^x}}. \quad (4.10)$$

Now, we consider the IR correlation function in the probe limit. Rewriting (4.7) in terms of the IR coordinate \bar{z} by using (3.21), χ in the IR region satisfies the following equation

$$0 = \partial_{\bar{z}}^2 \chi + \left(1 - \frac{2R_{IR}}{R_{UV}}\right) \frac{1}{\bar{z}} \partial_{\bar{z}} \chi + \frac{R_{IR}^2 m_\chi^2}{R_{UV}^2 \bar{z}^2} \chi \quad (4.11)$$

Solving this equation, the profile of χ reads in the IR region

$$\chi = \bar{c}_1 \bar{z}^{2R_{IR}/R_{UV} - \Delta_{IR}^x} + \bar{c}_2 \bar{z}^{\Delta_{IR}^x}, \quad (4.12)$$

where the IR conformal dimension is given by

$$\Delta_{IR}^x = \frac{R_{IR}}{R_{UV}} \Delta_{UV}^x = \frac{\sqrt{8\lambda}}{\sqrt{8\lambda + m_\phi^4}} \Delta_{UV}^x. \quad (4.13)$$

Comparing the IR solution with the UV one in (4.8), the integral constants are determined as

$$\bar{c}_1 = \left(\frac{R_{UV}}{R_{IR}^{R_{IR}/R_{UV}}}\right)^{2 - \Delta_{UV}^x} c_1 \quad \text{and} \quad \bar{c}_2 = \left(\frac{R_{UV}}{R_{IR}^{R_{IR}/R_{UV}}}\right)^{\Delta_{UV}^x} c_2. \quad (4.14)$$

Using the numerical values used in Fig. 4, the analytic IR conformal dimension in (4.13) reproduces the numerical result in (4.6).

In sum, we showed that the dual QFT of the interpolating geometry flows from the UV to IR fixed points with varying coupling constant and ground state. We also showed that the change of the ground state modifies the local operator's conformal dimension in the probe limit from Δ_{UV}^x to Δ_{IR}^x along the RG flow. Therefore, the IR two-point function is given by

$$\langle O_\chi(t, x_1) O_\chi(t, x_2) \rangle = \frac{1}{|x_1 - x_2|^{2\Delta_{IR}^x}}, \quad (4.15)$$

with the following IR conformal dimension

$$\Delta_{IR}^x = \frac{\sqrt{8\lambda}}{\sqrt{8\lambda + m_\phi^4}} \Delta_{UV}^x, \quad (4.16)$$

where the anomalous dimension of O_x is given by

$$\gamma_x \equiv \Delta_{IR}^x - \Delta_{UV}^x = - \left(1 - \sqrt{\frac{8\lambda}{8\lambda + m_\phi^4}} \right) \Delta_{UV}^x < 0. \quad (4.17)$$

5 Discussion

By applying the holographic method, in the present work, we have studied the momentum-space and real-space RG flows of a two-dimensional QFT from a UV to IR fixed point. To describe RG flows, we first assumed a relevant operator deforming a UV CFT to an IR CFT. On the dual gravity theory side, such an RG flow can be described by a geometric solution interpolating a local maximum to a minimum. More precisely, an unstable equilibrium point (or local maximum) with a negative potential energy corresponds to a UV fixed point of the dual QFT. Near this local maximum, the interpolating geometry is well approximated by an AdS space due to the restoration of conformal symmetry. On the other hand, a new IR fixed point of the RG flow maps to a stable equilibrium point (or local minimum) where another AdS space becomes a geometric solution. To see these features more clearly, we introduced a simple scalar potential as a toy model, which allows several local extrema. Then, we numerically found an interpolating geometry and explicitly showed that the coupling constant derived from the interpolating geometry has a vanishing β -function at UV and IR fixed points. These numerical results, as we mentioned before, indicate that the RG flow from a UV to IR fixed point can be represented by rolling a scalar field from an unstable to stable equilibrium point on the gravity theory side.

In general, a nonperturbative RG flow modifies a coupling constant and ground state of QFT, which also affects quantum correlations. Therefore, we expect that the entanglement entropy measuring the entanglement of the ground state nontrivially changes along the RG flow. On the interpolating geometry, we first studied the relation between the RG scale and the strength of the coupling constant from the momentum-space RG flow point of view. The relevant deformation allows the coupling constant to increase along the RG flow and makes IR physics nonperturbative. By applying the real-space RG flow description, we also investigated the RG flow of entanglement entropy. We first numerically studied the change of the nonperturbative entanglement entropy in the entire RG scale. After identifying the bulk scalar field with the coupling constant, we further represented the entanglement entropy

as a function of the coupling constant. This numerical result showed that the entanglement entropy logarithmically diverges at the UV and IR fixed points due to the restoration of the conformal symmetry. To understand the RG flow further, we also investigated the analytic behavior of the entanglement entropy near the fixed points. Using the perturbative expansions around $\phi = 0$ near the UV fixed point and $\phi = \phi_{IR}$ near the IR fixed point, we determined the analytic coupling constant dependence of the β -function, c -function, and entanglement entropy near the fixed points. We explicitly showed that the analytic calculation near the fixed points is perfectly matched to the nonperturbative numerical result.

We further studied the RG flow of a conformal dimension holographically. In the holographic setup, it was proposed that a two-point function in the probe limit can be described by a geodesic length connecting two local operators. After introducing additional local operators, we calculated their two-point functions following the holographic prescription. In this case, we assumed a probe limit where additional local operators do not modify the ground state because of weak interaction with the background matter. Even in this case, the change of the ground state affects the correlation function of the additional operators. Using this holographic method, we investigated the RG flow of a two-point function numerically when the ground state varies. The numerical result showed that the conformal dimension of a local operator in the probe limit monotonically decreases as the background coupling constant increases along the RG flow. To get more information about the change of the conformal dimension, we further studied the change of the two-point function analytically near the fixed points and evaluated the analytic anomalous dimension at the IR fixed point, which is perfectly matched to the previous numerical one.

Acknowledgement

C. P. was supported by the Mid-career Researcher Program through the National Research Foundation of Korea grant funded by the Korean government (No. NRF-2019R1A2C1006639). J. H. L. was supported by the National Research Foundation of Korea grant funded by the Korean government (No. NRF-2021R1C1C2008737)

References

- [1] J. M. Maldacena, *Adv. Theor. Math. Phys.* **2**, 231 (1998), [arXiv:hep-th/9711200](#) .
- [2] J. M. Maldacena, *Phys. Rev. Lett.* **80**, 4859 (1998), [arXiv:hep-th/9803002](#) .
- [3] E. Witten, *Adv. Theor. Math. Phys.* **2**, 253 (1998), [arXiv:hep-th/9802150](#) [hep-th] .
- [4] E. Witten, *Adv. Theor. Math. Phys.* **2**, 505 (1998), [,89(1998)], [arXiv:hep-th/9803131](#) [hep-th] .
- [5] S. S. Gubser, I. R. Klebanov, and A. M. Polyakov, *Nucl. Phys. B* **636**, 99 (2002), [arXiv:hep-th/0204051](#) .
- [6] O. Aharony, O. Bergman, D. L. Jafferis, and J. Maldacena, *JHEP* **10**, 091 (2008), [arXiv:0806.1218](#) [hep-th] .

- [7] I. R. Klebanov and G. Torri, *Int. J. Mod. Phys. A* **25**, 332 (2010), [arXiv:0909.1580 \[hep-th\]](#) .
- [8] J. de Boer, E. P. Verlinde, and H. L. Verlinde, *JHEP* **08**, 003 (2000), [arXiv:hep-th/9912012](#) .
- [9] M. Petrini and A. Zaffaroni, *PoS tnr99*, 053 (1999), [arXiv:hep-th/0002172](#) .
- [10] D. Z. Freedman, S. S. Gubser, K. Pilch, and N. P. Warner, *Adv. Theor. Math. Phys.* **3**, 363 (1999), [arXiv:hep-th/9904017](#) .
- [11] S. de Haro, S. N. Solodukhin, and K. Skenderis, *Commun. Math. Phys.* **217**, 595 (2001), [arXiv:hep-th/0002230](#) .
- [12] M. Bianchi, D. Z. Freedman, and K. Skenderis, *Nucl. Phys. B* **631**, 159 (2002), [arXiv:hep-th/0112119](#) .
- [13] R. C. Myers and A. Sinha, *JHEP* **01**, 125 (2011), [arXiv:1011.5819 \[hep-th\]](#) .
- [14] H. Casini, M. Huerta, R. C. Myers, and A. Yale, *JHEP* **10**, 003 (2015), [arXiv:1506.06195 \[hep-th\]](#) .
- [15] S. Gukov, *JHEP* **01**, 020 (2016), [arXiv:1503.01474 \[hep-th\]](#) .
- [16] E. Kiritsis, F. Nitti, and L. Silva Pimenta, *Fortsch. Phys.* **65**, 1600120 (2017), [arXiv:1611.05493 \[hep-th\]](#) .
- [17] J. K. Ghosh, E. Kiritsis, F. Nitti, and L. T. Witkowski, *JHEP* **05**, 034 (2018), [arXiv:1711.08462 \[hep-th\]](#) .
- [18] C. Park, D. Ro, and J. Hun Lee, *JHEP* **11**, 165 (2018), [arXiv:1806.09072 \[hep-th\]](#) .
- [19] U. Gürsoy, E. Kiritsis, F. Nitti, and L. Silva Pimenta, *JHEP* **10**, 173 (2018), [arXiv:1805.01769 \[hep-th\]](#) .
- [20] J. K. Ghosh, E. Kiritsis, F. Nitti, and L. T. Witkowski, *JHEP* **02**, 055 (2019), [arXiv:1810.12318 \[hep-th\]](#) .
- [21] C. Park and J. Hun Lee, *Phys. Rev. D* **101**, 086008 (2020), [arXiv:1910.05741 \[hep-th\]](#) .
- [22] S. Ryu and T. Takayanagi, *Phys. Rev. Lett.* **96**, 181602 (2006), [arXiv:hep-th/0603001 \[hep-th\]](#) .
- [23] S. Ryu and T. Takayanagi, *JHEP* **08**, 045 (2006), [arXiv:hep-th/0605073 \[hep-th\]](#) .
- [24] I. R. Klebanov, D. Kutasov, and A. Murugan, *Nucl. Phys. B* **796**, 274 (2008), [arXiv:0709.2140 \[hep-th\]](#) .
- [25] A. Karch, J. Maciejko, and T. Takayanagi, *Phys. Rev. D* **82**, 126003 (2010), [arXiv:1009.2991 \[hep-th\]](#) .
- [26] T. Takayanagi, *Phys. Rev. Lett.* **107**, 101602 (2011), [arXiv:1105.5165 \[hep-th\]](#) .
- [27] N. Ogawa, T. Takayanagi, and T. Ugajin, *JHEP* **01**, 125 (2012), [arXiv:1111.1023 \[hep-th\]](#) .
- [28] J. Erdmenger, M. Flory, C. Hoyos, M.-N. Newrzella, and J. M. S. Wu, *Fortsch. Phys.* **64**, 109 (2016), [arXiv:1511.03666 \[hep-th\]](#) .
- [29] J. Erdmenger, M. Flory, C. Hoyos, M.-N. Newrzella, A. O'Bannon, and J. Wu, *Fortsch. Phys.* **64**, 322 (2016), [arXiv:1511.09362 \[hep-th\]](#) .
- [30] M. Rangamani and T. Takayanagi, *Holographic Entanglement Entropy*, Vol. 931 (Springer, 2017) [arXiv:1609.01287 \[hep-th\]](#) .
- [31] T. Takayanagi and K. Umemoto, *Nature Phys.* **14**, 573 (2018), [arXiv:1708.09393 \[hep-th\]](#) .
- [32] G. Vidal, J. I. Latorre, E. Rico, and A. Kitaev, *Phys. Rev. Lett.* **90**, 227902 (2003), [arXiv:quant-ph/0211074](#) .
- [33] M. Levin and X.-G. Wen, *Phys. Rev. Lett.* **96**, 110405 (2006), [arXiv:cond-mat/0510613](#) .

- [34] M. Srednicki, *Phys. Rev. Lett.* **71**, 666 (1993), arXiv:hep-th/9303048 .
- [35] P. Calabrese and J. L. Cardy, *J. Stat. Mech.* **0406**, P06002 (2004), arXiv:hep-th/0405152 .
- [36] H. Casini, M. Huerta, and R. C. Myers, *JHEP* **05**, 036 (2011), arXiv:1102.0440 [hep-th] .
- [37] L. Susskind and E. Witten, (1998), arXiv:hep-th/9805114 .
- [38] S. N. Solodukhin, *Nucl. Phys. B* **539**, 403 (1999), arXiv:hep-th/9806004 .
- [39] E. D'Hoker, D. Z. Freedman, and W. Skiba, *Phys. Rev. D* **59**, 045008 (1999), arXiv:hep-th/9807098 .
- [40] H. Liu and A. A. Tseytlin, *Phys. Rev. D* **59**, 086002 (1999), arXiv:hep-th/9807097 .
- [41] V. Balasubramanian and S. F. Ross, *Phys. Rev. D* **61**, 044007 (2000), arXiv:hep-th/9906226 .
- [42] J. Louko, D. Marolf, and S. F. Ross, *Phys. Rev. D* **62**, 044041 (2000), arXiv:hep-th/0002111 .
- [43] P. Kraus, H. Ooguri, and S. Shenker, *Phys. Rev. D* **67**, 124022 (2003), arXiv:hep-th/0212277 .
- [44] L. Fidkowski, V. Hubeny, M. Kleban, and S. Shenker, *JHEP* **02**, 014 (2004), arXiv:hep-th/0306170 .
- [45] C. Park and J. H. Lee, *JHEP* **02**, 135 (2021), arXiv:2008.04507 [hep-th] .
- [46] D. Rodriguez-Gomez and J. G. Russo, *JHEP* **06**, 048 (2021), arXiv:2102.11891 [hep-th] .
- [47] C. Park, *Phys. Rev. D* **110**, 046010 (2024), arXiv:2405.15108 [hep-th] .
- [48] I. Peschel, M. Kaulke, and Ö. Legeza, *Annalen der Physik* **8** (1998).
- [49] K.-S. Kim, M. Park, J. Cho, and C. Park, *Phys. Rev. D* **96**, 086015 (2017), arXiv:1610.07312 [hep-th] .
- [50] P. Calabrese and J. L. Cardy, *Int. J. Quant. Inf.* **4**, 429 (2006), arXiv:quant-ph/0505193 .
- [51] N. S. Deger, *JHEP* **11**, 025 (2002), arXiv:hep-th/0209188 .
- [52] S. S. Gubser, *Adv. Theor. Math. Phys.* **4**, 679 (2000), arXiv:hep-th/0002160 .
- [53] C. Park, *Eur. Phys. J. C* **81**, 521 (2021), arXiv:2011.13555 [hep-th] .
- [54] C. Park, *Phys. Lett. B* **842**, 137978 (2023), arXiv:2209.07721 [hep-th] .
- [55] C. Park, S.-J. Kim, and J. H. Lee, *Mod. Phys. Lett. A* **39**, 2450004 (2024), arXiv:2212.01214 [hep-th] .
- [56] H. Kim, J. Pal, and C. Park, *Phys. Rev. D* **109**, 126019 (2024), arXiv:2312.12669 [hep-th] .